Organic Electronics 44 (2017) 115–119

Contents lists available at ScienceDirect

Organic Electronics

journal homepage: www.elsevier.com/locate/orgel

Letter

Emission from outside of the emission layer in state-of-the-art phosphorescent organic light-emitting diodes

R. Mac Ciarnain [a, b], D. Michaelis [a], T. Wehlus [c], A.F. Rausch [c], N. Danz [a, *], A. Bräuer [a], A. Tünnermann [a, b]

[a] *Fraunhofer Institute for Applied Optics and Precision Engineering IOF, Albert-Einstein-Str. 7, D-07743 Jena, Germany*
[b] *Institute of Applied Physics, ABBE Center of Photonics, Friedrich-Schiller-University Jena, Albert-Einstein-Str. 15, D-07745 Jena, Germany*
[c] *OSRAM OLED GmbH, Wernerwerkstr. 2, D-93049 Regensburg, Germany*

ARTICLE INFO

Article history:
Received 30 October 2016
Received in revised form
9 January 2017
Accepted 6 February 2017
Available online 7 February 2017

Keywords:
Organic light-emitting diode
Emission zone profile
In-situ characterization
Optical simulation

ABSTRACT

The emission zone profile in an organic light-emitting diode was extracted by fitting the experimentally measured far-field angular electroluminescence spectrum of a purposely designed device. It is based on a thin 10 nm emission layer doped with the red emitting phosphor $Ir(MDQ)_2acac$. We find strong indications for light emission originating from outside of the emission layer, even though the device has electron and hole blocking layers. These are commonly assumed to completely confine the charge carrier recombination and hence the light emission to the emission layer. Since the calculated internal spectrum of the emission matches the emitter photoluminescence spectrum well, diffusion of the emitter molecules outside of the emission layer is hypothesized.

The emission zone profile (EZP), i.e. the spatial density of photon emission events inside the active stack, is a crucial aspect to understanding the complex workings of an organic light-emitting diode (OLED). Knowledge of the EZP in an OLED can give information on charge transport and exciton diffusion [1–5], internal quantum efficiency (q) and efficiency roll-off [6–9], energy transfer between different emitters [10], emission color [11], material degradation and device lifetime [12] and is necessary for the latest emitter orientation extraction methods [13]. Previously, the EZP has been simulated using an electronic model [5,6,14–17], measured using sensing layers [2,11,18–20] which requires fabrication of many devices, and more recently by microcavity inverse light outcoupling approaches [13,21] using a single adapted microcavity device. A position accuracy of the EZP peak position of 1 nm has been claimed by introducing artificial noise to a model and then extracting the EZP by M. Carvelli et al. [22]. Alternatively, as will be further discussed below, EZP spatial resolution limited to the first three eigenfunctions of the corresponding singular value decomposition problem was found for a 10 nm wide emission zone [23].

This work reports emission pattern measurements that cannot be quantitatively described by light emission originating from the emissive layer (EML) only. A widening of the EZP into the blocking layers, which should confine charges to the emission layer (Fig. 1(c)), yields a simulation result that fits the experimental pattern. Earlier, OLEDs without blocking layers have been reported to have emission originating from outside the emission layer [20,24]. However, for a state-of-the-art device with blocking layers this has never before been contemplated in the literature.

The EZP extraction method used in this work is that described by Flämmich et al. [13]. The EZP of the OLED is modelled by a set of normalized weights for discrete emission positions. These weights are determined by fitting the sum of the simulated angular emission spectra from each emission location in the device to the experimentally measured angular electroluminescence (EL) spectrum. Only TE polarized light is considered here, which is emitted only by emitter transition dipole moment components parallel to the interfaces. Therefore, the effect of emitter orientation distribution is negligible and material birefringence has no effect on our results. An electron transport layer (ETL) thickness (~the cathode-emitter distance) of 160 nm has been selected to yield a microcavity interference minimum in the emission spectra, as can be seen running from the top left to the bottom right of Fig. 1(a). Here, the majority of light containing little information on the EZP is

* Corresponding author.
E-mail address: norbert.danz@iof.fraunhofer.de (N. Danz).

http://dx.doi.org/10.1016/j.orgel.2017.02.006
1566-1199/

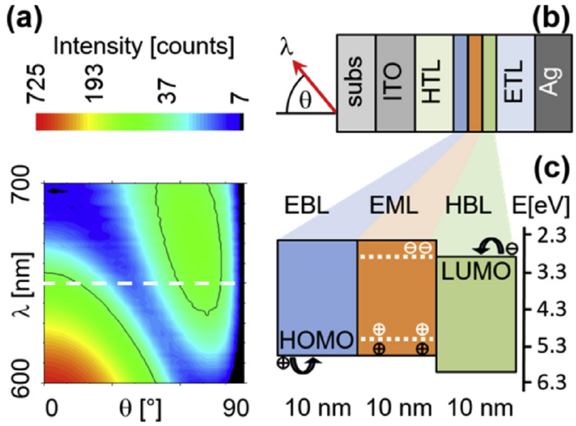

Fig. 1. Device characteristics with the measured TE polarized experimental spectrum is plotted in (a). A white dashed line marks the wavelength $\lambda = 650$ nm. Part (b) is a sketch of the device layer structure, featuring a glass substrate, an ITO anode, hole transporting (HTL), electron blocking (EBL), emission (EML), hole blocking (HBL), electron transporting (ETL) layers and an Ag cathode. The red arrow illustrates the observation direction at angle θ from the normal to the stack interfaces. Part (c) shows the electron/hole LUMO and HOMO energy levels for the EBL, EML and HBL. White dashed lines and symbols are for the emitter dopant and black lines and symbols are for the hosts. Circles enclosing a minus and a plus show likely electron and hole buildup respectively. (For interpretation of the references to colour in this figure legend, the reader is referred to the web version of this article.)

suppressed, leaving mostly light sensitive to EZP changes. Singular value decomposition breaks down the resolution of the detectable EZP into a sum of constant, linear, quadratic, cubic etc. terms of the eigenfunctions. Following [23] and using our measurement system dynamic range (~280), the first three eigenfunctions (EF) of the EZP shape can be resolved. So the spatial resolution is limited to the sum of a constant, linear and quadratic function. Higher order EZP functions cannot be resolved due to the limited signal to noise ratio (SNR) of our measurements.

The OLED structure is shown in Fig. 1 and comprises a 10 nm thick EML and electron blocking layer (EBL), both composed of α-NPD, but the EML with 3% $Ir(MDQ)_2acac$ emitter doping concentration. α-NPD is a good hole transporter [25] but holes are also energetically likely to jump to the low concentrated emitters, so holes can be present towards the anode side of the EML, too. $Ir(MDQ)_2acac$ has electron transporting properties at 10% concentration [12], but worse at our 3% concentration. Diez et al. [10] state that at low concentrations (5%) similar to our device holes and electrons accumulate more to the cathode side of the EML, but that the EZP extends fully across 11 nm of the EML.

Layer thicknesses have been extracted from spectral reflectivity measurements performed after each layer deposition step as well as with the complete device. The EL emission pattern has been measured at 5 mA/cm^2 using spectral discretization of 2 nm (the resolution of our fiber and spectrometer detection system) from 600 nm to 700 nm, as per Fig. 1(a), the most sensitive region to EZP changes. Angular step width was set to 4° (with an angular resolution of 3° determined by the distance from the OLED to the fiber).

The quality of the fit will be described by the relative root mean square RMS_{rel} that is defined by

$$RMS_{rel} = \frac{\left[\frac{1}{N}\sum_{k,l}\left[I_{\exp}(\theta_k,\lambda_l) - I_{sim}(\theta_k,\lambda_l)\right]^2\right]^{1/2}}{\left[\frac{1}{N}\sum_{k,l}\Delta I(\theta_k,\lambda_l)^2\right]^{1/2}}. \quad (1)$$

It compares the RMS deviation of the experimental I_{exp} to the simulated I_{sim} intensities with the RMS deviation given by the error ΔI of the experimental data. This error includes alignment of OLED center to the center of rotation of the measurement system and angular resolution limitations (in sum ±1% intensity) plus detection noise of 1 count intensity. RMS_{rel} is calculated from the entire measured wavelength and angular range as in Fig. 1(a), and not just at a single wavelength or single observation angles as shown in

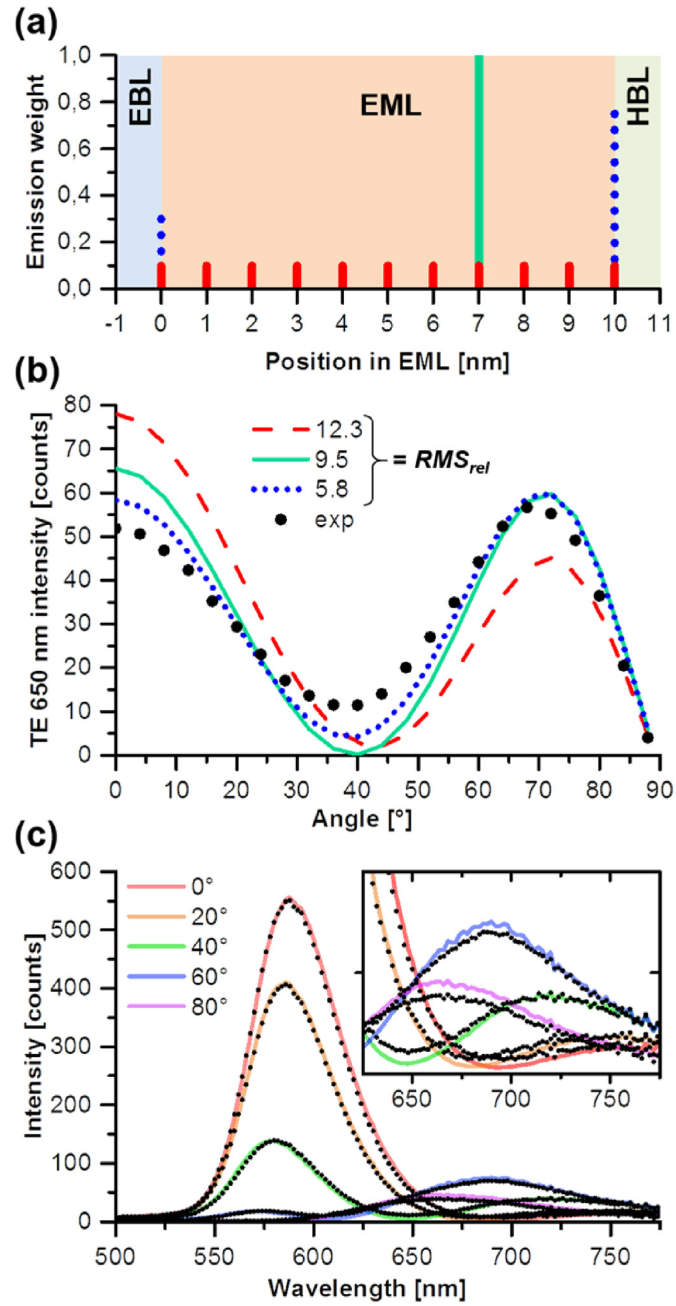

Fig. 2. Data fitting assuming EML emission only. (a) plots idealized EZPs that are constant (short red lines), single position (long green line) and edge only (dotted blue lines). (b) shows the resulting simulated angular intensity patterns using these EZPs along with experimental data (black circles) for 650 nm TE emission. The experimental noise level is 1 count. The legend gives the RMS_{rel} values for the fitted spectra but calculated over the full wavelength range. Diagram (c) shows spectral data observed at five different observation angles (black dots) along with the corresponding simulation results for the interface-only EZP, where the long wavelength part has been magnified in the inset. (For interpretation of the references to colour in this figure legend, the reader is referred to the web version of this article.)